Photoproduction of Pions in Carbon*

T. R. PALFREY, B. M. K. NEFKENS,† L. MORTARA, AND F. J. LOEFFLER
Department of Physics, Purdue University, Lafayette, Indiana
(Received December 23, 1960)

Positive and negative pions were produced by photons on a carbon target and observed at laboratory angles of 35°, 73°, and 121°. At each angle the yield of mesons of constant energy was observed by a magnetic spectrometer as a function of peak bremsstrahlung energy. Seven values of the latter ranging from 205 to 335 Mev were used. Yields and π^-/π^+ ratios corrected for various systematic experimental errors are presented. By using a photon difference method the bremsstrahlung spectra were unfolded from the yield curves to give meson cross sections versus photon energy at fixed pion energies. These functions are compared with predicted yields which consider the internal momentum distribution of the target nucleons; the agreement is adequate.

I. INTRODUCTION

THE following work was begun primarily as a monitoring measurement during an experiment to measure the photoproduction of pions from deuterium at energies near threshold. We decided to explore the photo-pion production from carbon further when it became apparent that: (1) Sufficient accuracy was possible to allow unfolding the bremsstrahlung spectrum by the photon difference method[1] to obtain the meson yield as a function of photon energy; (2) A large fraction of the events appeared to correspond to processes in which the residual nucleus was left with a large amount of excitation energy (i.e., much more energy than the nucleus would receive in a simple two-body event). This was also observed by Crowe *et al.*[2] Because of (1) above, it is possible to explore this point quantitatively by comparing the observed yield with that expected when the internal momenta of the nucleons in the carbon nucleus are considered.[3] The strictly two-body process from carbon has been observed in another experiment at this laboratory by detecting the beta decays of the two residual nuclei, B^{12} and N^{12};[4] (3) There was a definite decrease of the π^-/π^+ ratio (to values less than 1 in some cases) as the energy of the photon producing the pion decreased. While this ratio for a complex nucleus depends in a nontrivial way on Coulomb barrier effects, nuclear binding, the scattering of outgoing mesons, and Pauli principle limitations on final nucleon states, semi-quantitative deductions may be possible from this information.

Photomesons from complex nuclei have been detected by many workers in a variety of ways.[5–8] We used a magnetic spectrometer to momentum-analyze the mesons produced at angles of 35°, 73° and 121° in the laboratory system; these correspond to center-of-mass angles of 45°, 90°, and 135° for a two-body reaction. The mean meson energy accepted by the spectrometer at each angle was chosen to be equal to the energy of pions produced from free nucleons by 200-Mev photons.

Yields of positive and negative pions were measured at each angle as a function of peak bremsstrahlung energy. Seven values were used covering a range from 205 to 335 Mev. Since the resolution function of the spectrometer is known, and since the photon difference method is feasible here, it is possible to obtain the absolute cross section for π^+ and π^- production from carbon as a function of angle and photon energy.

II. EXPERIMENTAL ARRANGEMENT

The bremsstrahlung beam used in this experiment was obtained from the Purdue synchrotron, which has a peak electron energy of 335 Mev and uses a platinum-wire target 0.040-in. thick. It was assumed that the photon spectrum was that described by Schiff[9] for a thick target. The energy calibration was based on measurements of the threshold for the photoproduction of mesons in hydrogen, and the use of a "Multiar" voltage comparator which measured the integral of dB/dt and hence B at any time in the magnet gap.[10] The photon yield varied from about 3×10^7 to 10^8 effective quanta per second over the range from 200 to 300 Mev.

The monitor used was a thick-walled ionization chamber of the Cornell type. It has been calibrated at Purdue and cross checked at the National Bureau of Standards Betatron Laboratory.[11]

The apparatus was arranged as shown in Fig. 1. The beam was collimated by a tapered lead collimator whose exit dimensions were $\frac{9}{16}$ in.$\times\frac{3}{4}$ in., this being followed

* This work was supported in part by the U. S. Atomic Energy Commission.
† Fulbright Travel Grant recipient from Rijksuniversiteit, Utrecht, The Netherlands.
[1] A. S. Penfold and J. E. Leiss, University of Illinois Internal Report, 1958 (unpublished).
[2] K. M. Crowe, R. M. Friedman, and H. Motz, Phys. Rev. **99**, 673 (1955).
[3] M. Lax and H. Feshbach, Phys. Rev. **81**, 189 (1951).
[4] G. W. Tautfest and F. J. Loeffler (private communication).
[5] A rather complete survey of literature pertaining to the photoproduction of pions up to 1956 is given by Carol M. Newton, Stanford University High-Energy Physics Laboratory Report, HEPL-100 (unpublished).
[6] W. R. Hogg and D. Sinclair, Phil. Mag. **1**, 466 (1956).
[7] W. S. C. Williams, K. M. Crowe, and R. M. Friedman, Phys. Rev. **105**, 1840 (1957).
[8] J. R. Waters, Phys. Rev. **113**, 1133 (1959).
[9] L. I. Schiff, Phys. Rev. **70**, 87 (1946).
[10] G. W. Tautfest and R. Fessel (to be published).
[11] F. J. Loeffler, T. R. Palfrey, and G. W. Tautfest, Nuclear Instr. **5**, 50 (1959).

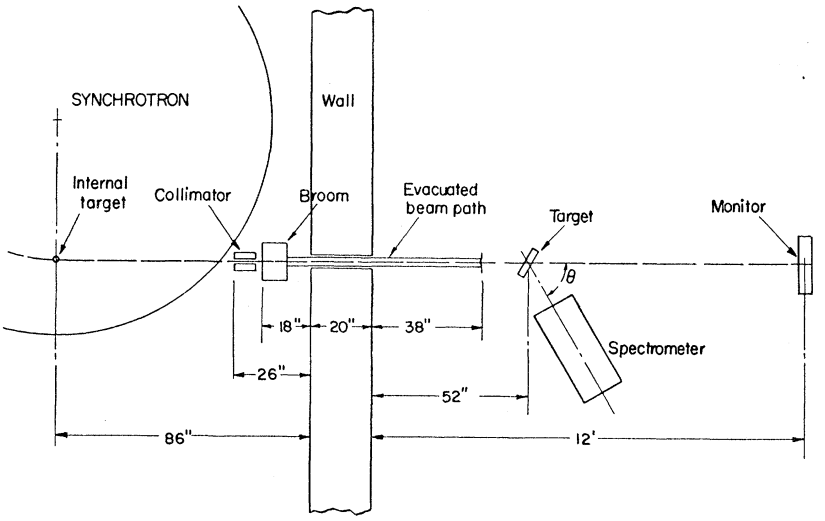

FIG. 1. Experimental arrangement.

by a broom magnet, and an evacuated pipe which enclosed the collimated beam to within 14 in. of the target. The beam passed through a wall of barite-loaded concrete 20 in. thick which shielded the spectrometer from the entire synchrotron, and then struck the target mounted on the axis of rotation of the spectrometer. Finally came the beam monitor.

The spectrometer used to deflect the mesons into the counter system is a 120° double-focusing, $n=0.5$ magnet with a mean radius of curvature of 18 in., radial aperture of 5 in., and mean gap spacing of 2.25 in. It is operated with the source position at 18 in. normal to the middle of the entrance gap, and with the detector plane 24.5 in. straight back from the entrance gap, and normal to the mean exit trajectory. The detection plane is thus not in the focal plane of the spectrometer, in fact lying somewhat within it for all but the lowest momentum particles. This configuration was chosen in order to make pion range measurements possible, to reduce and simplify decay-in-flight and multiple-scattering corrections, and to reduce the physical size of the counters.

In this geometry, the resolution of each of the five defining counters is about 5% in momentum. The resolution of the whole system (corresponding to lumping the counts from all five momentum channels) is shown in Fig. 2. This resolution function includes effects of the finite size of the source and the energy-dependent parts of the decay in flight and multiple-scattering corrections described below. It has been obtained by numerical integration of orbits through the spectrometer, using the known magnetic field and a program written for the Purdue Burroughs 205 digital computer. There are two additional broadenings of the resolution function in this experiment which were not included in the figure. One is an increase in the full width of about 10% due to finite target thickness, and the other is an additional increase of less than 10% due to multiple scattering in the first two counters in the detection system.

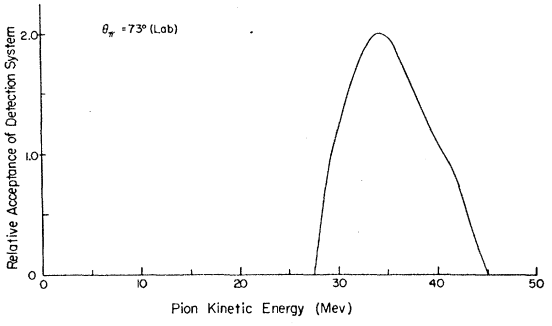

FIG. 2. Magnetic spectrometer resolution function.

The angular resolution of the spectrometer in the laboratory was constant at ±4°, full width at half maximum.

Seven plastic scintillation counters were used to detect the π mesons. For meson laboratory angles of 35° and 73°, two scintillators ($\frac{1}{4}$ in. thick) constituted counters $C1$ and $C2$ which formed a telescope at the exit of the spectrometer. Some pulse-height discrimination was possible at this point but the primary purpose of the telescope was to insure that particles counted in the five rear counters ($C3$–$C7$) did indeed come through the spectrometer. At the backward angle (121° in the lab) $C1$ was removed because the electron background was low enough to make it unnecessary and also because the π mesons at this angle had quite low energies (~22 Mev) which would have been degraded excessively in the two-counter telescope. At this angle, nearly all mesons were stopped in the rear counters.

Five energy bins were defined by counters $C3$–$C7$ placed approximately in the focal plane of the spectrometer. Each counter was $3\frac{1}{4}\times3\frac{1}{4}\times\frac{3}{4}$ in. thick and was viewed by an RCA 6810 A photomultiplier. A block diagram (Fig. 3) depicts the counters and the counting electronics schematically. The pulses from the anode of each photomultiplier were clipped by a shorted stub to 15 mμsec. Signals from $C1$ and $C2$ were then

immediately put into a fast coincidence circuit of 12 mμsec resolving time.

Signals from the rear counters, $C3$ through $C7$, were fed into discriminators $D3$ through $D7$. These units were voltage discriminators using a pair of EFP-60's in the trigger circuit and providing a fast (15 mμsec rise; 65 mμsec wide) standard pulse-out. The fast discriminator outputs were each put in coincidence ($C123$ through $C127$) with the output of the fast $C12$ coincidence circuit except at the backward angle (121° lab) where $C1$ was not used, and $C2$ took the place of the double-coincidence signal $C12$.

The resolving times of the $C12n$ circuits were checked by varying the length of cable between the rear counters and their discriminators and obtaining delay curves. The mesons for these measurements came from a Be target which was used as a relatively prolific meson source for calibration purposes. All scaling channels were gated on only during the 1–5 msec bremsstrahlung pulse.

In order to discriminate against electrons in the back counters it was necessary to determine the pulse-height distribution in these counters. This was done according to the scheme shown in Fig. 4. Pulses to be analyzed were taken from the last dynode of the desired phototube, linearly mixed with a gate generated by any desired combination of pulses, and pulse-height analyzed.

The most serious problem in the identification of mesons concerned the separation of electron and meson pulses. This was especially difficult at the forward angle (35° lab) where electrons were abundant. There was a pulse-height difference of approximately 50% in the rear counters for electrons and pions of mean momentum. The finite momentum and pulse-height resolution of the spectrometer and the counters, and the Landau tails in the energy loss lead one to expect an overlap of the electron and pion pulse-height distributions.

This indeed was the case and the dashed curve in Fig. 5 shows the situation for a Be target and rear counter $C6$ with the discriminator $D6$ set very low. Two

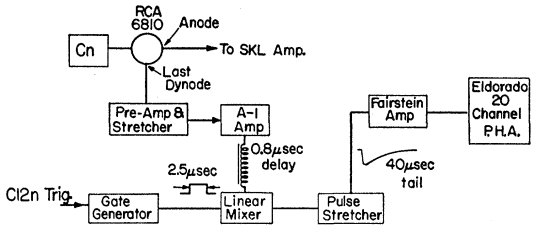

FIG. 4. System for measuring pulse height spectra in individual counters.

distinct bumps are evident in the $C6$ pulse-height distribution (a $C126$ signature is here required to trigger the analyzer) and suggest electron and meson groups. In order to verify this, runs were also made with a Cd target which would produce relatively many electrons compared to mesons. Results are shown by the solid curve in Fig. 5. As expected, the supposed electron bump became quite large compared to the meson bump, but the overlap of electron and meson distributions is also quite obvious.

As a further test Lucite absorbers were placed in front of the rear counters. As the absorber thickness was increased the electron peak remained stationary and the meson peak shifted toward larger pulse height, again as expected, since the electrons of appropriate momentum to get through the spectrometer are minimum ionizing. This separation was desirable and as a compromise between excessive scattering and effective separation of electron and meson peaks, absorbers in the neighborhood of 1-in. thickness were used in front of all the rear counters. Figure 6 shows a typical pulse-height distribution obtained in the rear counters ($C4$ in this case) with the Lucite absorber in place. In practice, after a distribution of this sort had been obtained, the pulse-height discriminator for that counter was set so as to exclude electron pulses and pass meson pulses. The arrow marked "disk set" in Fig. 6 illustrates the discrimination level chosen for counter 4. This determination was done by eye, and clearly either a few mesons are lost or a few

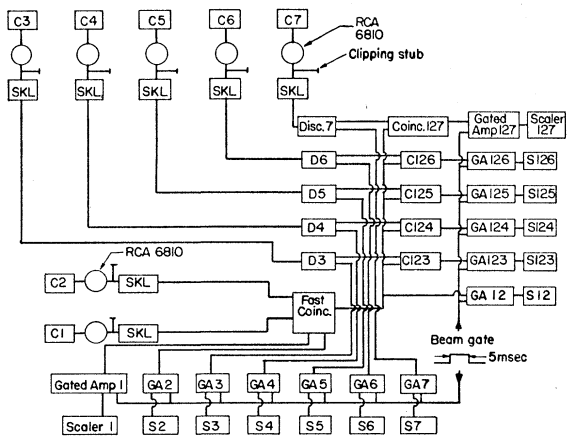

FIG. 3. Block diagram of counting electronics.

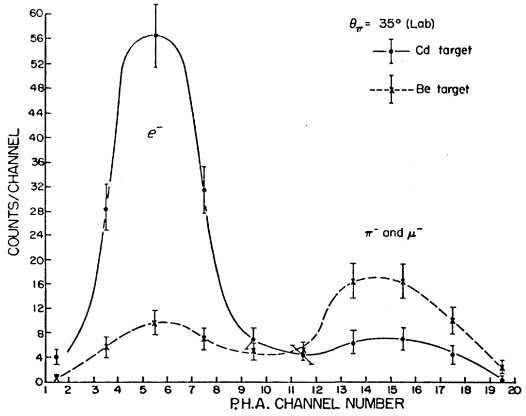

FIG. 5. Pulse height distribution in $C6$ for Be and Cd targets with discriminator $D6$ set at zero.

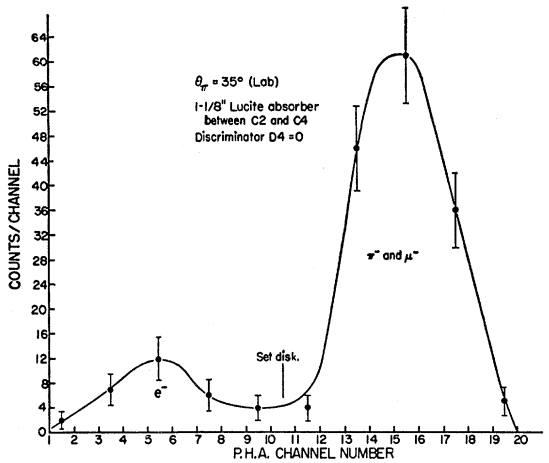

FIG. 6. Pulse height distribution in $C4$ for a Be target and a Lucite absorber placed in front of $C4$.

electrons gained, but we feel confident that the worst mistake made for meson detection at the forward angle (35° lab) was ±2% in the number of mesons counted. To first order this mistake cancels in measuring the π^-/π^+ yield, since there are equal numbers of electrons and positrons, and of course very nearly equal numbers of π^- and π^+ mesons produced in the target. The absolute yields of either π^- or π^+ will, however, carry this error in them. The situation at 73° and 121° was better because the separation of electron and meson pulse heights was greater. The error in the number of mesons counted at these angles was less than 1% because of this effect.

Since $C1$ and $C2$ were not used with discriminators during the 35° and 73° runs it was necessary to set their gains by adjusting the phototube high voltage. As expected, a fairly large region or plateau was found where the rear counter rate was independent of $C1$ and $C2$ high voltages. In order to keep the single rates in $C1$ and $C2$ low to reduce the chance coincidence rate, $C1$ and $C2$ high voltages were set near the low end of the plateau region. At the backward angle (121° lab) only $C2$ was used ahead of the rear counters and it was provided with a discriminator for convenience. The appropriate bias level was selected in a manner similar to the one described above.

After pulse-height distributions were obtained for each of the rear counters and all bias levels were selected, the counting rates in each counter were observed with a ThC″ source placed in a standard position. During the run, the ThC″ rates were checked each day and gains adjusted if necessary. Also, pulse-height spectra were measured for each rear counter several times during the experiment as an extra precaution.

Between data runs, we took background runs by measuring the yield without target. Within statistics, the background proved to be independent of the charge sign of the pion and of peak bremsstrahlung energy. We measured also the π^- yield at 73° at various peak bremsstrahlung energies with a 2-in.-diam liquid hydrogen target and the π^+ yield below threshold with the same target. Both yields were, within statistics, the same as the background.

TABLE I. Fraction of the mesons counted in the spectrometer, which are actually muons, as a function of angle and peak bremsstrahlung energy.

θ_π (lab)	35°		73°		121°	
k_0 (Mev)	330	218	330	205	330	205
Fraction	8±3%	7±3%	8.5±3%	6±3%	8±3%	10±3%

III. CORRECTIONS

A. π^- Stars

In the measurement at 121° the pions stopped in the scintillator or very close to it in the light pipe of a rear counter. Stopped negative pions give rise to stars and star particles could give a count in a neighboring counter. A 1% effect was measured in agreement with a theoretical estimate. The π^- yield curve at 121° was corrected for this.

B. Decay in Flight

In traveling from the target to the rear counters, an appreciable number of mesons decayed. This effect was calculated and it was found that the fraction of mesons which decayed before reaching the rear counters was: 28% at 35°, 34% at 73°, and 40% at 121°. This is partly compensated by the fact that decay muons, when

TABLE II. Yield/effective quantum, corrected for decay in flight. The uncertainty in this correction, ±10%, is not included in the quoted uncertainty. The yield of π^- at 121° is also corrected for 1% "star-counts."

k_0 (Mev)	π^+	π^-
	35°	35°
326	(1.31 ±0.04) ×10^{-9}	(1.61 ±0.05) ×10^{-9}
312	(1.25 ±0.04) ×10^{-9}	(1.48 ±0.05) ×10^{-9}
279	(0.98 ±0.03) ×10^{-9}	(1.18 ±0.04) ×10^{-9}
246	(0.68 ±0.02) ×10^{-9}	(0.73 ±0.02) ×10^{-9}
230	(0.47 ±0.018)×10^{-9}	(0.48 ±0.02) ×10^{-9}
218	(0.216±0.009)×10^{-9}	(0.211±0.009)×10^{-9}
	73°	73°
335	(1.37 ±0.05) ×10^{-9}	(1.86 ±0.05) ×10^{-9}
304	(1.21 ±0.04) ×10^{-9}	(1.56 ±0.05) ×10^{-9}
279	(0.97 ±0.04) ×10^{-9}	(1.37 ±0.04) ×10^{-9}
246	(0.67 ±0.02) ×10^{-9}	(0.79 ±0.03) ×10^{-9}
230	(0.42 ±0.02) ×10^{-9}	(0.54 ±0.02) ×10^{-9}
218	(0.25 ±0.01) ×10^{-9}	(0.29 ±0.01) ×10^{-9}
205	(0.112±0.008)×10^{-9}	(0.101±0.008)×10^{-9}
	121°	121°
326	(0.82 ±0.02) ×10^{-9}	(1.31 ±0.04) ×10^{-9}
304	(0.75 ±0.02) ×10^{-9}	(1.10 ±0.03) ×10^{-9}
279	(0.63 ±0.02) ×10^{-9}	(0.93 ±0.03) ×10^{-9}
246	(0.422±0.015)×10^{-9}	(0.59 ±0.02) ×10^{-9}
230	(0.282±0.010)×10^{-9}	(0.436±0.014)×10^{-9}
218	(0.180±0.007)×10^{-9}	(0.260±0.009)×10^{-9}
205	(0.107±0.006)×10^{-9}	(0.146±0.008)×10^{-9}

going in the proper direction and having the proper momentum, will be counted as pions. In order to make the appropriate decay-in-flight corrections to the data, it is necessary to find how many muons are counted. These numbers were calculated using a reasonable incident pion spectrum[12] and are given in Table I. The meson yields corrected for decay in flight and π^- stars are presented in Table II.

C. Nuclear Absorption

To be counted the mesons had to traverse, on the average, half of the target thickness, a small amount of air and Mylar, and the counters and absorbers placed at the exit of the spectrometer. Estimates of the nuclear attenuation in the various absorbers and counters and in the target have been made for each angle. In the target it was assumed that only highly inelastic processes would change the net number of pions in the beam; and in the counters and absorbers behind the magnet, it was assumed that essentially any nuclear scattering would prevent the pion from being counted. Appropriate geometric cross sections were used, and no differentiation between positive and negative pion cross sections was made. On these assumptions, the pion loss due to nuclear scattering was 11% at 35°, 6% at 73°, and 3% at 121°.

D. Multiple Scattering Losses

The large separation between the counters at the exit of the spectrometer magnet and the five momentum defining counters gave rise to significant multiple scattering losses. These losses were nearly all in one plane and so are readily estimated from multiple scattering theory. The loss of particles due to multiple scattering was 9% at 35°, and 15% each at the other two angles.

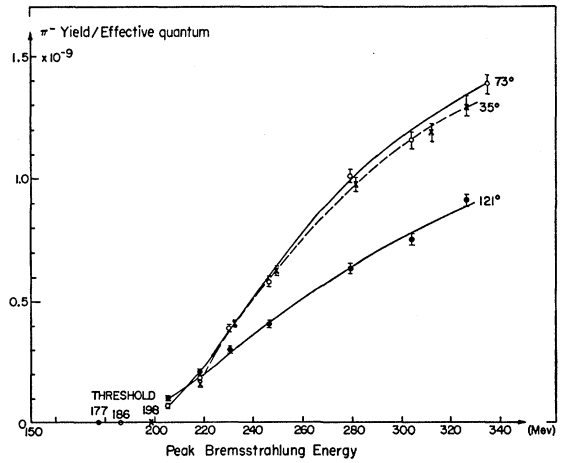

FIG. 7. The π^- yield as a function of peak bremsstrahlung energy.

[12] J. M. Peterson, W. S. Gilbert, and R. S. White, Phys. Rev. 81, 1003 (1951).

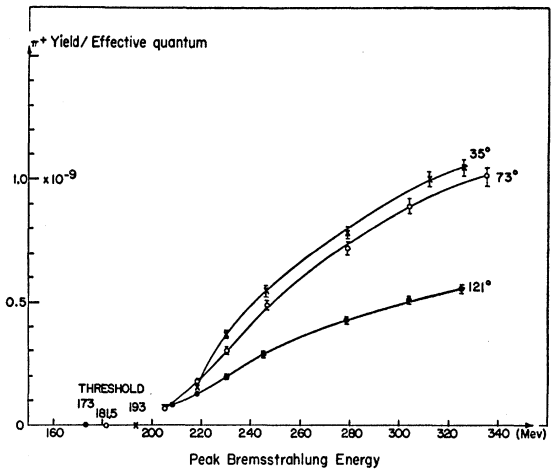

FIG. 8. The π^+ yield as a function of peak bremsstrahlung energy.

These figures may overestimate the effect by as much as 30% of the correction because of failure to take precisely into account the poorly known angular and spacial spread of the meson beam as it entered the counters in which it scattered.

IV. EXPERIMENTAL RESULTS

The yield per effective quantum for π^- production at the three angles, as a function of peak bremsstrahlung energy, is plotted in Fig. 7 and for π^+ in Fig. 8. The curves are corrected for background only. From the measured π^- and π^+ yields, we have calculated the π^-/π^+ ratios and plotted them as a function of the peak bremsstrahlung energy in Fig. 9.

The photon-difference method of Leiss and Penfold was used to reduce the yield curves as a function of peak bremsstrahlung energy to differential cross sections. The cross sections obtained are $d^2\sigma/d\Omega dT_\pi$ cm^2-sr^{-1}-Mev^{-1} as a function of photon energy, and these are shown in Figs. 10–12. The spectrometer resolution function has not been unfolded from the results—it being rather more direct to put the resolution function into the theoretical predictions in making the comparison between the theory discussed in the subsequent section and the results. Errors are not shown in the photon-difference results but are discussed below.

The yield points which were photon-differenced were widely spaced, but of quite good statistical accuracy. Except near threshold, no strong energy dependence of the minus-plus ratio was measured. The resolution function of the spectrometer was sufficiently broad so that no fine structure in the differential cross section could have been measured. Consequently the data were treated as follows: The results for positive and negative pions were averaged, the yield curve was plotted, then differentiated at evenly spaced points. The derivative was smoothed by visual fit, and reintegrated to give a smooth yield curve. The tables of Leiss and Penfold

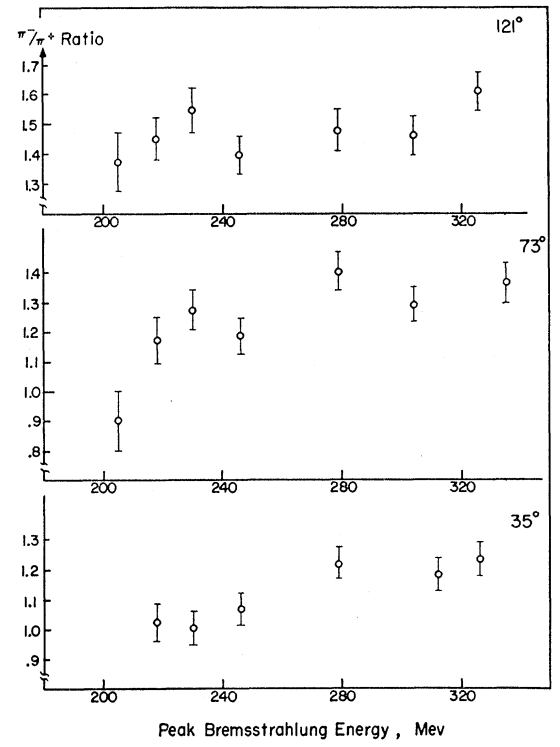

FIG. 9. The π^-/π^+ ratios as a function of peak bremsstrahlung energy for the three angles.

were then used to perform the photon-differencing operation. With such a procedure it is perhaps most meaningful to discuss errors in terms of other yield curves which could reasonably have been drawn through the same data points. Using this criterion, we would attach errors of 15–20% to the magnitude of the differential cross section in the tail of the curve, and errors of 12–15% in the region of the maximum. The peculiar curvatures of the 35° and 73° cross sections in the neighborhood just beyond the peak of the cross section are presumably of statistical origin, and therefore require no physical explanation.

Systematic errors in beam calibration or any other error which varies with peak bremsstrahlung energy can give particularly misleading results in the measurement of slowly varying tails such as those in the differential cross sections deduced from the data of this experiment.

TABLE III. The efficiency ϵ, for π^+ production per proton in carbon compared to production from free protons.

k_0 (Mev)	θ_π (lab)	ϵ
205	73°	0.077±0.007
218	73°	0.104±0.007
230	73°	0.16 ±0.01
246	73°	0.25 ±0.02
279	73°	0.35 ±0.02
326	121°	0.36 ±0.04

TABLE IV. The π^-/π^+ comparison with other experiments.

Reference	k_0 (Mev)	Angle (lab)	Mean T_π (Mev)	Method	π^-/π^+
14	330	26°		Emulsions	1.03±0.25
17	310	30°	54	Magnet and counters	1.22±0.07
12	335	45°	70	Emulsions	1.34±0.20
13	335	90°	30–150	Emulsions	1.7 ±0.2
12	335	90°	56	Emulsions	1.30±0.12
14	330	90°		Emulsions	1.43±0.13
16	320	90°		Magnet and vel. sel.	1.27±0.06
17	310	90°	34	Magnet and counters	1.22±0.07
17	310	90°	70	Magnet and counters	1.18±0.08
12	330	135°	54	Emulsions	1.34±0.20
15	310	135°	65±15	Magnet and counters	1.06±0.02
17	310	180°	44	Magnet and counters	1.26±0.10
17	310	180°	62	Magnet and counters	1.18±0.13

Two such effects are present in these measurements: pole-face scattering, and muon contamination. We estimate that the systematic errors from improper calculation of the muon contamination, from pole-face scattering, and from beam calibration inaccuracies do not vary by as much as 5% from 200 to 330 Mev peak bremsstrahlung energy. A uniformly varying 5% systematic error (i.e., an error that is 0% at 200 Mev, rising linearly to 5% at 330 Mev peak bremsstrahlung energy) would change the magnitude of the high-energy tail of the differential cross-section by only about 15%.

A somewhat interesting comparison between π^+ production from carbon and hydrogen can be made by evaluating the relative efficiency ϵ, for production per proton in carbon compared to production from a free proton. Table III gives this efficiency as a function of peak bremsstrahlung energy for two laboratory angles. The hydrogen data at 73° was obtained with a liquid-hydrogen target at this laboratory and a CH_2 target and a subtraction method were used for the 121° data.

V. DISCUSSION OF RESULTS

A. The Minus-Plus Ratio

In Fig. 9 it can be noted that the minus-plus ratio rises with peak bremsstrahlung energy and with laboratory angle.

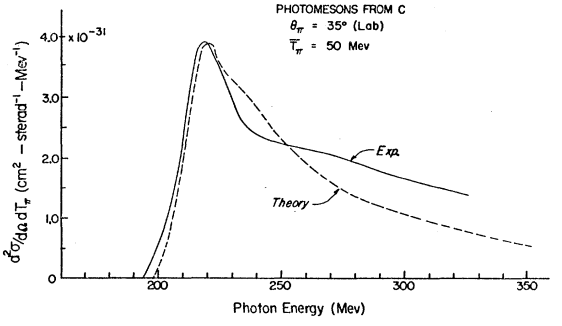

FIG. 10. Differential cross section for π^+ and π^- production from carbon at 35° as a function of photon energy.

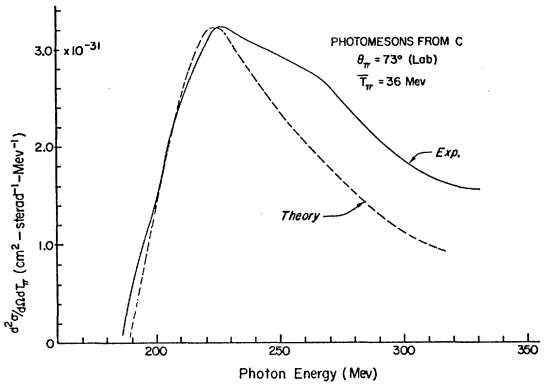

FIG. 11. Differential cross section for π^+ and π^- production from carbon at 73° as a function of photon energy.

The dependence on peak bremsstrahlung energy is what one expects from the difference in thresholds for production of positive and negative pions at the energies and angles observed. The mass difference between B^{12} and N^{12}, the energetically least expensive final states in charged photoproduction from carbon, is about 4.2 Mev. A shift of the yield curves relative to each other along the peak bremsstrahlung energy axis by the difference in masses is sufficient to remove most of the variation with respect to peak bremsstrahlung energy. Coulomb effects are relatively unimportant at the pion energies observed. These would tend to affect the absolute magnitude of the minus-plus ratio, rather than its dependence on peak bremsstrahlung energy, since the Coulomb interactions are primarily with the residual nucleus, the relative momentum of which should change only gradually with photon energy.

The angular dependence of the minus-plus ratio is similar to that observed in photoproduction from deuterium, namely, that which would approximately be anticipated from free nucleons. That this free-nucleon minus-plus ratio is qualitatively maintained is consistent with the results of the model calculation in the next paragraphs, and gives confidence to calculations of meson-production from nuclei in which the meson production from free nucleons is used as the starting point. A comparison with minus-plus ratios obtained in other experiments[12–17] is made in Table IV.

B. The Differential Cross Section

The theoretical approach of Lax and Feshbach[3] was used in an attempt to fit the dependence of the differential cross sections on photon energy. Their explanation is based entirely on a model of photoproduction from a single nucleon. The initial momentum vector of this nucleus is allowed to vary because of the internal momentum distribution within the target nucleus. Energy and momentum are still conserved in this theory of the production process. The known resolution function of the detection apparatus of this experiment was folded into the results of Lax-Feshbach type calculations for the angles and energies of pions measured. The momentum distribution used was the same as that in their original paper, namely $N(p)dp \propto p^2(\alpha^2+p^2)^{-2}dp$, where p is the nucleon momentum, and α was chosen as 185 Mev/c. The theoretical curves are shown with the experimental results in Figs. 10–12. The theoretical curves were normalized to the peak of the experimental curves, but were in no other way adjusted.

The agreement between the experiment and the predictions of the simple model are good. The principal disagreement is in the rate of decrease of the differential cross section at high photon energies. Although the errors in the photon-differencing of the experimental results are large, they are not sufficient to explain the consistently high value of the experimental results. Furthermore, the power-law behavior of the theoretical momentum spectrum used in the calculation would tend to overestimate the high-momentum part of the internal nucleon momentum distribution, and would consequently overestimate the cross section at high photon energies. Therefore this disagreement is real. We believe this tail is a contribution of two-step processes not included in the model of Lax and Feshbach: The high-energy photon produces a high-energy meson which scatters (internally in the parent nucleus) into the pion energy and angular bin in which we are counting. This scattering inherently prevents measurement of the internal momentum distribution of nucleons in a nucleus by photoproduction experiments of the type presented here.

It should be added that the differential cross section shows no evidence for processes in which the final

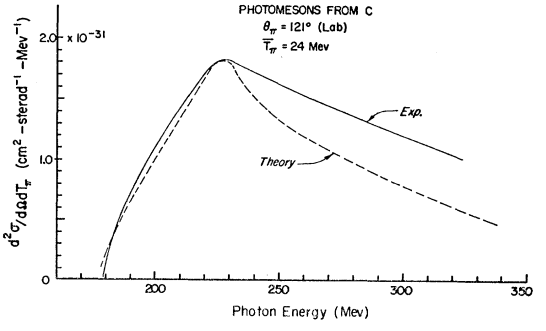

FIG. 12. Differential cross section for π^+ and π^- production from carbon at 121° as a function of photon energy.

[13] E. M. McMillan, J. M. Peterson, and R. S. White, Science **110**, 579 (1950).
[14] B. F. Feld, D. H. Frisch, I. L. Lebow, L. S. Osborne, and J. S. Clark, Phys. Rev. **85**, 680 (1952).
[15] R. M. Littauer and D. Walker, Phys. Rev. **86**, 838 (1952).
[16] J. E. Carothers, Phys. Rev. **92**, 538(A) (1953).
[17] P. D. Luckey, Phys. Rev. **97**, 469 (1955).

nucleus is either B^{12} or N^{12} in a particle-stable state. (These reactions are kinematically distinguishable, and would lead to a bump on the rising edge of the differential cross-sections in Figs. 10–12). From the data we can say that these processes therefore amount to less than about 10% of the total pion photoproduction cross-section from carbon at 200 Mev photon energy.

ACKNOWLEDGMENTS

We wish to recognize here the assistance of Professor H. R. Fechter in several phases of the experiment. Mr. R. Fessel developed much of the electronics used and aided in numerous other ways. Mr. D. Johnson and the synchrotron crew provided steady beams and assisted in taking data.

PHYSICAL REVIEW VOLUME 122, NUMBER 4 MAY 15, 1961

Comparison of the Scattering of Positrons and Electrons from Nuclear Charge Distributions*

GEORGE H. RAWITSCHER
Yale University, New Haven, Connecticut

AND

C. RUTHERFORD FISCHER
New Mexico State University, Las Cruces, New Mexico

(Received January 3, 1961)

Elastic scattering cross sections of 183-Mev positrons and electrons are calculated for various charge distributions of the Ca and Au nuclei. It is shown that the combined use of positron and electron scattering measurements can lead to a determination of the nuclear charge distribution which is more accurate than that derived from either one of the scattering cross sections when used by itself. The scattered particles obey Dirac's equation and the nuclei are assumed to be static spherically symmetric charge distributions, whose radial dependence is given in terms of a three-parameter family of curves.

I. INTRODUCTION

A GREAT deal of information concerning the dependence of nuclear charge density on radial distance has been achieved in the last years,[1] in particular by the high-energy electron scattering experiments.[2] The charge density is determined with highest accuracy at the nuclear surface, near the "halfway point," a certain amount of ambiguity still remaining at the central and tail regions. Positrons may prove useful in resolving such uncertainties because, due to repulsion rather than attraction of the wave function from the center of the nucleus, the different regions of the nuclear charge distribution should affect the cross section with weights differing from those in the case of electrons.[3]

This work is an attempt to establish the nature and extent of such positron-electron differences in a rough exploratory fashion. Cross sections of positrons and electrons scattered by nuclei having various spherical charge distributions are calculated numerically. The radial dependence of the nuclear charge distributions considered in this work is given in terms of three parameters and can be made to vary continuously from a "wine-bottle" to a Woods-Saxon form. The effect on the electron scattering cross section produced by a change in the form of the nuclear charge distribution is compared to the corresponding effect on the positron cross section. Conclusions are drawn regarding the reduction of the inaccuracy in the determination of the charge distribution from the combined e^+ and e^- scattering experiments and analyses. Incidentally, refinement of this type of investigation might ultimately permit the detection of effects which are usually neglected in the calculations, for instance, the deformation from sphericity which could occur during the scattering.

In Sec. III a comparison between the electron and positron cross sections is made for four shapes of the charge distribution of Ca. Two of the charge distributions (WB–1 and WB–2) have various central wine-bottle-like depressions, and are intended to furnish a comparison of sensitivity of electron and positron scattering to the internal regions of the nucleus. The two other charge distributions (WS–1 and WS–2) have no central depression but differ instead by 6% in their surface thickness. The nucleus chosen is Ca because in this case the numerical inaccuracies in the cross section are estimated to be small compared to the effect due to the changes of the charge distribution.

Two other charge distributions are considered for the nucleus of Au. The effects are sizable in this case, but

* This research was supported by the U. S. Air Force under a contract monitored by the Air Force Office of Scientific Research of the Air Research and Development Command.

[1] K. W. Ford and D. L. Hill, Ann. Rev. Nuclear Sci. **5**, 25 (1955).

[2] R. Hofstadter, Ann. Rev. Nuclear Sci. **7**, 231 (1957).

[3] The authors are indebted to Professor G. Breit for bringing this point to their attention. Compare also with footnote 12.